POLSAR TIME SERIES PROCESSING AND ANALYSIS BASED ON BINARY PARTITION TREES

Alberto Alonso-González, Carlos López-Martínez, and Philippe Salembier

Universitat Politècnica de Catalunya (UPC), Dept. of Signal Theory and Communications (TSC), Jordi Girona 1-3, 08034, Barcelona, Spain. E-mail: alberto.alonso@tsc.upc.edu

ABSTRACT

This paper deals with Polarimetric Synthetic Aperture Radar image time series exploitation. A Binary Partition Tree (BPT) is proposed to process this data. The BPT is a region-based and multi-scale data representation that contains useful information about the data structure at different detail levels. Two different alternatives are proposed for modeling the target behavior in the temporal dimension leading to distinct BPT representations. Both approaches are analyzed and discussed and some examples of possible BPT-based applications are presented. These sample applications are employed to process a real RADARSAT-2 time series dataset to exemplify its capabilities.

Key words: SAR, PolSAR, Segmentation, Time series, Speckle filtering, Binary Partition Tree.

1. INTRODUCTION

During the past years some space-borne Polarimetric Synthetic Aperture Radar (PolSAR) missions have become operative, making possible the collection of image time series datasets. These datasets contain some acquisitions of the same scene at different time instants, making possible not only a better characterization about the scene, but also about its temporal evolution.

However, the analysis and interpretation of SAR images is difficult due to the presence of speckle. The speckle is produced by the coherent processing of the SAR image focusing, conforming a combination of all the individual targets within a resolution cell, resulting in a grainy appearance over distributed targets that is refered to as *speckle noise*. Note that the speckle is a true electromagnetic measure but, due to its complexity, it is considered as noise and, consequently, it must be characterized statistically.

To deal with PolSAR image interpretation we propose to employ the Binary Partition Tree (BPT) [8] as a data abstraction. This structure will be defined in Section 2, whereas on Section 3 it will be discussed how it may be extended to deal with time series datasets. Section 5 will present some results with real data and Section 6 will describe some applications to analyze the temporal information. Finally, some conclusions about the proposed technique are discussed in Section 7.

2. BINARY PARTITION TREE

The Binary Partition Tree (BPT) was introduced in [8] in the context of image processing as a region-based and multi-scale image representation. It is a hierarchical representation conforming a binary tree where each node represents a connected region of the image that is composed by the merging of its two child nodes. As a consequence, the leaves of the tree may be considered as the individual pixels of the image whereas the root node of the tree represents the whole image. Between them, there are a wide number of nodes represent regions of the image at different detail levels. This representation contains useful information about the scene structure at different scales that may be useful for a range of applications.

Data processing based on the BPT representation may be decomposed into two basic steps: BPT construction and BPT exploitation, as presented on Fig. 1. BPT construction is the generation of the tree structure from the original data. Since it only exploits internal relationships within the data, it may be seen as application independent. A representation of the BPT construction is shown on Fig. 2. On the other hand, when the BPT has been constructed, it has to be exploited for a particular application. A tree pruning is proposed in [8] as the extraction of the *useful* or *interesting* regions from within the tree. As this depends on the particular application, this step is application dependent.

Recently, the BPT has been extended to process PolSAR images [1] and hyperspectral images [9][5]. For PolSAR data, it has demonstrated to be a useful data abstraction for speckle filtering and segmentation, being able to extract homogeneous regions of the image of very different sizes while also preserving the spatial resolution

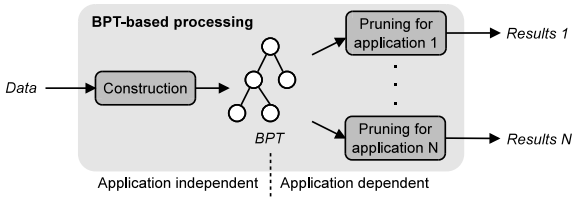

Figure 1: BPT-based processing scheme.

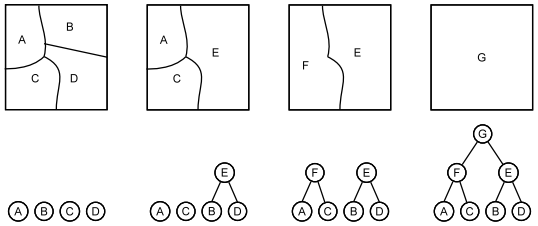

Figure 2: BPT construction example with 4 initial regions.

and small details [4]. In this paper the extension of this BPT structure to process temporal series of PolSAR images is addressed, presenting a comparison of two different approaches depending on target characterization on the temporal domain.

3. TIME SERIES BPT

In order to extend the BPT representation to the temporal dimension, two different approaches are presented, based on the temporal characterization of the target that is assumed:

- On the one hand, it may be assumed that a target is completely characterized by the polarimetric response and, consequently, a change in terms of its polarimetric response among the temporal dimension may be assumed as a target change. On this approach, the temporal dimension is just another additional dimension of the data, leading to a three-dimensional Space-Time BPT (ST BPT) representation.
- On the other hand, the target response may be supposed to follow a particular *temporal evolution* among the temporal dimension. Therefore a target is characterized by the complete polarimetric temporal evolution among all the acquisitions. On this approach, the temporal dimension is employed as an additional feature of the target characterization, resulting in a tree representing spatial regions with similar polarimetric temporal evolution. In the following, this representation is referred to as Temporal Evolution BPT (TE BPT).

As proposed on [8], the BPT may be constructed by an iterative algorithm in a bottom-up approach. Starting from the original pixels, at each iteration the two most similar adjacent regions are merged until the root of the tree is generated. In order to apply this algorithm, the following elements have to be defined in order to be able to construct the BPT from the original data.

3.1. Region model

Each node of the BPT is populated with a region model that represents all the pixels of the region it embodies. It should be representative enough for all the applications on that the BPT is intended to be used. For the ST BPT, the same region model as for a PolSAR image BPT may be employed, as proposed on [2], corresponding to the PolSAR covariance matrix

$$\mathbf{Z} = \langle \mathbf{k}\mathbf{k}^H \rangle_n = \frac{1}{n}\sum_{i=1}^{n} \mathbf{k}_i \mathbf{k}_i^H \tag{1}$$

where $\mathbf{k}_i$ represents the scattering vector of the *i*-th pixel, n represents the number of pixels of the region and ^{H} represents the complex hermitian transpose.

For the TE BPT, the temporal dimension should be included within the region model, as this is part of the target characterization. Consequently, an extended region model $\mathbf{Z}_e$ is employed

$$\mathbf{Z}_e = \langle \mathbf{k}_e \mathbf{k}_e^H \rangle_n = \begin{pmatrix} \mathbf{Z}_{11} & \mathbf{\Omega}_{12} & \cdots & \mathbf{\Omega}_{1N} \\ \mathbf{\Omega}_{12}^H & \mathbf{Z}_{22} & \cdots & \mathbf{\Omega}_{2N} \\ \vdots & \vdots & \ddots & \vdots \\ \mathbf{\Omega}_{1N}^H & \mathbf{\Omega}_{2N}^H & \cdots & \mathbf{Z}_{NN} \end{pmatrix} \tag{2}$$

where N represents the number of acquisitions of the dataset, $\mathbf{Z}_{ii}$ is a 3 by 3 covariance matrix representing the polarimetric information of the *i*-th acquisition, as expressed in (1), and $\mathbf{\Omega}_{ij}$ is a 3 by 3 complex matrix representing the correlation between the acquisitions *i* and *j*.

3.2. Data connectivity

As mentioned before, the BPT representation contains connected regions of the data at different scales. A data connectivity has to be defined for both approaches, since they are representing regions on different domains. For the ST BPT, the 10 connectivity is employed in the space-time domain, as represented on Fig. 3. Each pixel is connected with the 8 neighbors on the same acquisition and with the pixels on the same position from the acquisitions just before and after.

On the TE evolution BPT, since it is a spatial data representation, the classical 8 connectivity may be employed, as shown on Fig. 4.

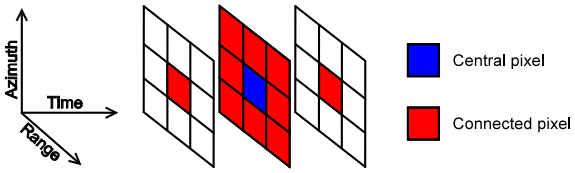

Figure 3: Space-Time BPT pixel connectivity.

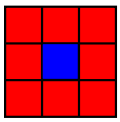

Figure 4: Temporal Evolution BPT pixel connectivity.

3.3. Similarity measure

The proposed BPT construction algorithm is based on the iterative merging of the most similar adjacent regions. Therefore, a similarity measure between regions has to be defined. This measure should be defined on the region model space, involving two different measures for the proposed representations. However, a generic extension of the similarity measure is proposed to take into account the temporal evolution of the extended model presented in (2).

Different similarity measures where proposed and analyzed for a single PolSAR image BPT construction in [3], where the geodesic similarity measure d_{sg}, based on the positive definite matrix cone geometry [6], resulted into the best results

$$d_{sg}(X,Y) = \left\| log\left(\mathbf{Z}_X^{-1/2}\mathbf{Z}_Y\mathbf{Z}_X^{-1/2}\right)\right\|_F + ln\left(\frac{2n_xn_y}{n_x+n_y}\right) \quad (3)$$

where $\mathbf{Z}_X$ and $\mathbf{Z}_Y$ represent the estimated covariance matrices for regions X and Y, respectively, n_x and n_y represent their number of pixels, $\|.\|_F$ represents the Frobenius matrix norm, $log(.)$ represents the matrix logarithm and $ln(.)$ represents the natural logarithm.

The geodesic similarity measure (3) is employed for the ST BPT construction process, whereas for the TE BPT an extension of this measure is proposed to take into account the complete polarimetric temporal evolution. This extended d_{eg} is based on comparing all the pairs of $\mathbf{Z}_{ii}$ matrices for both regions based on the d_{sg} measure

$$d_{eg}(X,Y) = \sqrt{\sum_{i=1}^{N}\left\| log\left(\mathbf{Z}_{X_{ii}}^{-1/2}\mathbf{Z}_{Y_{ii}}\mathbf{Z}_{X_{ii}}^{-1/2}\right)\right\|_F^2 + } + ln\left(\frac{2n_xn_y}{n_x+n_y}\right) \quad (4)$$

where $\mathbf{Z}_{X_{ii}}$ represents the $\mathbf{Z}_{ii}$ component of the X region, as shown on (2). The same idea may also be applied to extend other similarity measures.

Note that both similarity measures exploit all the polarimetric information under the Gaussian hypothesis.

4. BPT PRUNING

As mentioned in Section 2, the BPT exploitation may be performed by a tree pruning process. This process looks for the useful or interesting nodes for a particular application within the tree. For speckle filtering and segmentation [4] it may be useful to look for the largest homogeneous regions on the scene. This process involves, then, the definition of a homogeneity measure ϕ for both BPTs. The pruning criterion is defined by imposing a threshold δ_p over this measure.

For the ST BPT the relative error homogeneity measure may be employed, as for the case of a single PolSAR image BPT pruning, since the same region model is used

$$\phi(X) = \frac{1}{n_x}\sum_{i=1}^{n_x}\frac{\|\mathbf{Z}^i - \mathbf{Z}_X\|_F^2}{\|\mathbf{Z}_X\|_F^2} < \delta_p \quad (5)$$

where $\mathbf{Z}^i$ is the estimated covariance matrix for the *i*-th pixel within region X, having n_x pixels, and δ_p is the pruning factor, usually expressed in dB.

For the TE BPT an extension of this measure to the whole temporal evolution may be applied. Accordingly, the extended homogeneity measure ϕ_e may be defined as

$$\phi_e(X) = \frac{1}{n_x}\sum_{i=1}^{n_x}\frac{\sum_{j=1}^{N}\|\mathbf{Z}_{jj}^i - \mathbf{Z}_{X_{jj}}\|_F^2}{\sum_{j=1}^{N}\|\mathbf{Z}_{X_{jj}}\|_F^2} < \delta_p \quad (6)$$

where $\mathbf{Z}_{jj}^i$ is the $\mathbf{Z}_{jj}$ covariance matrix for the *i*-th pixel within region X and $\mathbf{Z}_{X_{jj}}$ is the $\mathbf{Z}_{jj}$ covariance matrix of the region model $\mathbf{Z}_e$ for the X region.

The homogeneity measures defined in (5) and (6) may be seen as the relative Mean Squared Error (MSE) that is committed when representing all the pixels of a region by its region model. Consequently, all the pruned regions of the BPT will be the largest regions having a relative MSE below the pruning threshold δ_p.

5. RESULTS

The proposed BPT representations have been employed to process a real RADARSAT-2 dataset consisting of 8 Full-Pol images acquired at FQ13 ascending mode from Flevoland, The Netherlands. This dataset was acquired during the ESA AgriSAR 2009 campaign, devoted to analyze the agricultural fields with PolSAR. The acquisition dates range from April 4th, 2009 to September 29th, 2009 with an acquisition every 24 days. From the whole data a cut of 4000 by 2000 pixels have been selected and coregistered, as shown on Fig. 5.

Results after processing the dataset with the proposed BPT structures are shown on Fig. 6. Due to the difficulties to represent the whole dataset, only the results over the first acquisition are shown. Note, however, that

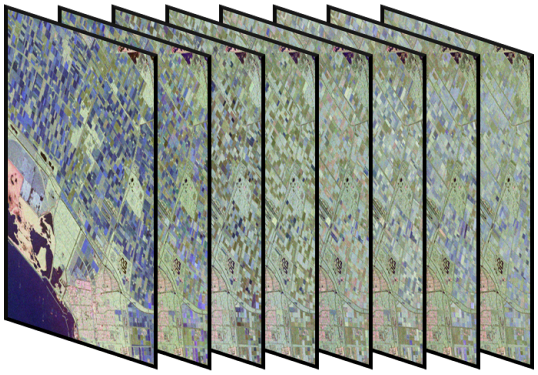

Figure 5: Flevoland dataset with 8 acquisitions in Pauli representation.

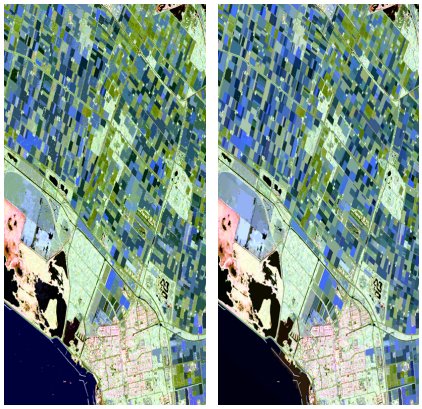

(a) ST BPT, ϕ (b) TE BPT, ϕ_e

Figure 6: Pauli representation for the first acquisition after processing the full dataset with the Space-Time BPT and the Temporal Evolution BPT employing $\delta_p = -3dB$.

the entire dataset has been processed, employing the time series representations presented on Section 3.

Comparing Figs. 6a and 6b, similar results are observed, but, if results are examined closely, some differences in terms of the region contours appear, as it may be seen on Fig. 7, where a detailed are is shown over the second acquisition. More contours appear within the agricultural fields in Fig. 7b and the spatial contours of the fields are not as clearly defined as in Fig. 7c. Note, in fact, that both results are not fully comparable since the two different BPT representations contain regions that are characterized in a different manner, as described in Section 3. The additional contours within fields obtained by the ST BPT are probably caused due to temporal contours, since some parts of the fields are connected with regions in acquisitions before or after. This effect may not be observed in TE BPT since it contains spatial (two-dimensional) regions. On the other hand, the spatial contours are more clearly defined in the TE BPT since an increase on contrast may be seen when comparing the whole polarimetric temporal evolution of the region in front of just the response from one acquisition. To see clearly this differences between the two BPT approaches,

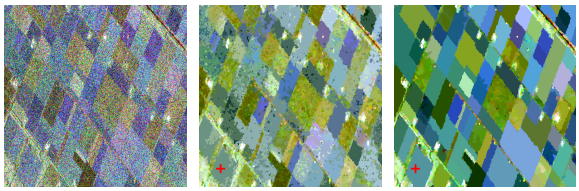

(a) Original (b) ST BPT, ϕ (c) TE BPT, ϕ_e

Figure 7: Pauli representation for a crop of the second acquisition after processing the full dataset with the ST BPT and the TE BPT for $\delta_p = -3dB$.

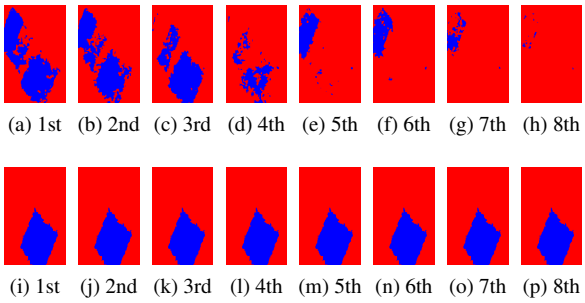

(a) 1st (b) 2nd (c) 3rd (d) 4th (e) 5th (f) 6th (g) 7th (h) 8th

(i) 1st (j) 2nd (k) 3rd (l) 4th (m) 5th (n) 6th (o) 7th (p) 8th

Figure 8: Region contours over all the acquisitions of the region marked in Fig. 7b, employing the ST BPT (first row) and for the region marked in Fig. 7c, employing the TE BPT (second row).

Fig. 8 shows the region shapes of the regions marked in Figs. 7b and 7c. As explained before, the regions contained within the ST BPT have arbitrary shapes in the space-time domain, whereas the TE BPT contains spatial regions corresponding to the same scene area on all the acquisitions.

In order to see the maintenance of the polarimetric information of these processed images, the H/A/$\bar{\alpha}$ polarimetric decomposition [7] is employed to compare the retrieved parameters with the ones obtained with the 7x7 multilook filter. Results are shown on Fig. 9 for the second acquisition area shown on Fig. 7a.

Similar values are obtained in terms of the H/A/$\bar{\alpha}$ parameters for the BPT approaches with respect to the multilook filter. Additionally, their ability to obtain large regions corresponding to the agricultural fields improves the polarimetric information estimation and reduces considerably the effects of the speckle noise, as it may be seen specially over the anisotropy (A) parameter. Moreover, Fig. 10 shows the temporal evolution of these parameters among the 8 different acquisitions for an agricultural field of the image. Once again, very similar trends are observed for the multilook and for the BPT-based approaches, indicating that the polarimetric temporal evolution is also preserved.

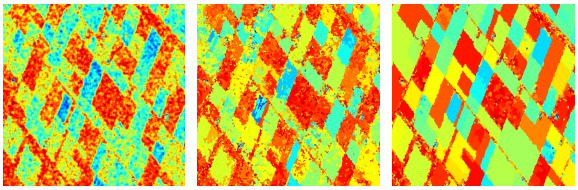

(a) 7x7 ML, H (b) ST BPT, H (c) TE BPT, H

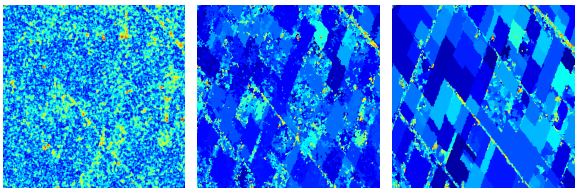

(d) 7x7 ML, A (e) ST BPT, A (f) TE BPT, A

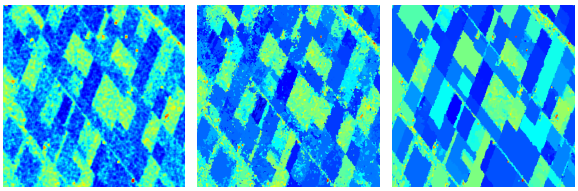

(g) 7x7 ML, $\bar{\alpha}$ (h) ST BPT, $\bar{\alpha}$ (i) TE BPT, $\bar{\alpha}$

Figure 9: H/A/$\bar{\alpha}$ parameters of the area presented in Fig. 7a after processing the full dataset with the ST BPT and with the TE BPT for $\delta_p = -3dB$.

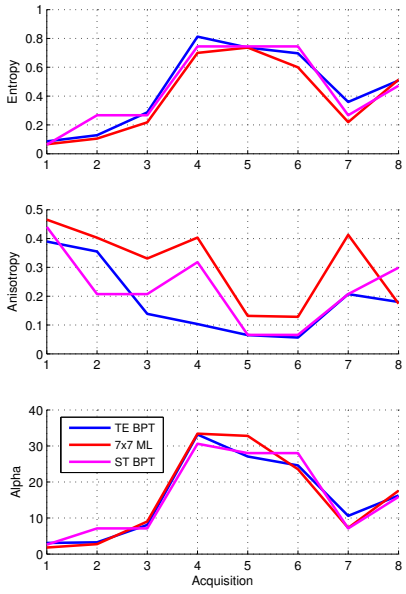

Figure 10: H/A/$\bar{\alpha}$ parameters evolution for an agricultural field. The full dataset has been processed with the TE BPT, with the 7x7 multilook filter and with the ST BPT employing $\delta_p = -3dB$.

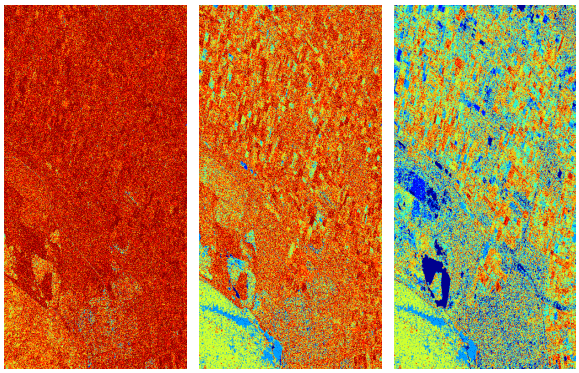

(a) $\delta_p = -5dB$ (b) $\delta_p = -3dB$ (c) $\delta_p = -1dB$

Figure 11: Number of temporal changes for different pruning factors δ_p. No changes is represented in blue and 7 changes in red.

6. TEMPORAL ANALYSIS

On the previous Section, the capabilities of the proposed PolSAR time series BPT representations to detect and characterize homogeneous regions on these datasets have been shown. In this Section some applications are depicted to show how the temporal information may be extracted and analyzed from within these regions of the tree. However, they are just some examples to show the potentialities of this time series data analysis. In fact, the exploitation of these datasets is a big challenge that is now starting to be studied and developed.

The ST BPT, as mentioned in Section 3, characterizes a target by its polarimetric response and, consequently, a change on its response is considered as a target change resulting in a temporal contour. As proposed on [2], the change detection application arises automatically when analyzing these temporal contours. A map may be generated showing the number of contours on the temporal dimension, indicating the number of temporal changes among all the acquisitions. Fig. 11 shows these maps for different pruning factors over the Flevoland dataset. As it may be seen, increasing the pruning factor results into larger regions in the temporal dimension, appearing with a smaller number of temporal contours on Fig. 11. This observation is consistent with [1], where the same behavior was observed when processing a single PolSAR image. As one may expect, the number of changes over the agricultural areas are larger, which is more clear in Fig. 11c, for large values of δ_p.

The results shown on Fig. 11 give an idea of the number of changes of the different parts of the scene. However, there is no indication about the *relevance* or *importance* of these changes. Moreover, due to the arbitrary shapes of the regions in the space-time domain, as shown on Figs. 8a-8h, these maps appear noisy since the regions cannot be tightly related to a particular area of the scene on all the acquisitions. To circumvent these limitations of the analysis based on the ST BPT, another temporal

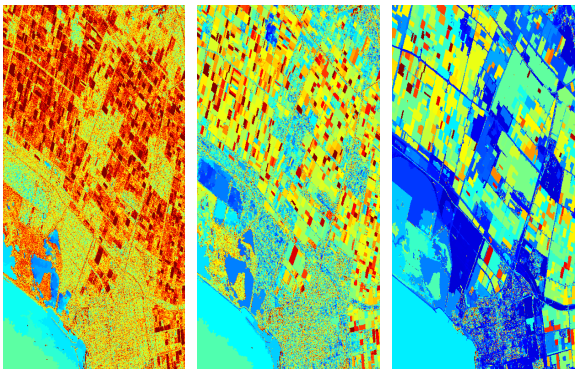

(a) $t_s, \delta_p = -5dB$ (b) $t_s, \delta_p = -3dB$ (c) $t_s, \delta_p = -1dB$

Figure 12: Temporal stability measure t_s for different pruning factors δ_p. $ts = 0$ is represented in blue and $t_s = 2.5$ in red.

analysis is proposed based on the TE BPT. Note that, on this representation, the regions can be clearly related to particular areas of the scene, since it contain spatial regions. As there are no temporal contours on the TE BPT, a temporal stability measure t_s is proposed over the extended model (2) to measure the relevance of the temporal changes among all the acquisitions $\mathbf{Z}_{ii}$

$$t_s = \frac{2}{N(N-1)} \sum_{i=1}^{N} \sum_{j=i+1}^{N} \left\| log\left(\mathbf{Z}_{ii}^{-1/2} \mathbf{Z}_{jj} \mathbf{Z}_{ii}^{-1/2}\right) \right\|_F . \tag{7}$$

The t_s measure defined in (7) may be seen as the average geodesic similarity measure [6] between all pair of acquisitions of the dataset. A region presenting low values of t_s indicates that the area of the scene it represents has not changed significantly in terms of polarimetric response between all the acquisitions and vice-versa. Fig. 12 represents the t_s measure over the Flevoland dataset for the same pruning factors as Fig. 11. It may be clearly seen that the changes produced in the agricultural areas are more relevant in terms of the polarimetric target response, resulting in larger t_s. Similar trends are observed when varying δ_p: for larger values of the pruning threshold smaller values are obtained for t_s due to the larger amount of speckle filtering and the consequent reduction of the polarimetric changes caused by the speckle noise. However, since large values of δ_p also produce larger regions, an homogeneous regions mixture may be produced for very large values of δ_p, resulting into an incorrect result of the t_s measure since the estimated region models may be no longer valid.

Note that these change detection and temporal stability applications are based on the similarity measures defined before, which are sensitive to the full polarimetric information under the Gaussian hypothesis. As a consequence, these applications are naturally sensitive to all this information.

7. CONCLUSIONS

In this paper the extension of the BPT data representation to PolSAR time series has been addressed. Two different approaches to deal with the temporal dimension of the data have been proposed. These approaches have been presented from the conceptual point of view of the target temporal characterization resulting, then, general enough to be applied for the extension of other methods to time series data.

The Space-Time BPT (ST BPT) is the extension of the BPT when assuming that a target is characterized by a particular polarimetric response. This approach results in dealing with the temporal dimension as an additional independent dimension of the data. Consequently, this structure may extract 3-dimensional space-time regions of the data having similar polarimetric response. It has a large amount of flexibility, being able to represent, for instance, regions with contours that are not fixed over time. However, its flexibility may produce some problems when interpreting the results, as the regions can not be clearly related to a specific scene area.

On the other hand, if it is assumed that the polarimetric response of a target follows an intrinsic temporal evolution, this temporal information may be employed to extend the target characterization resulting in the Temporal Evolution BPT (TE BPT). This approach extracts 2-dimensional spatial regions of the scene following a similar polarimetric temporal evolution. It is easier to interpret than the ST BPT since its regions are uniquely related to a particular scene area but it may not be able to properly represent regions having not fixed contours over time. However, probably most of the region contours over land may be considered fixed. Moreover, this extended target characterization allows a better contrast within regions producing more precise region contours.

These BPT structures may be useful for different applications involving PolSAR time series exploitation. As examples, two different applications have been defined to detect temporal changes and to measure the polarimetric temporal stability of the scene regions. Nevertheless, the full polarimetric information may be extracted to analyze and interpret the temporal evolution of the scene, which may be useful for many applications in the future.

ACKNOWLEDGMENTS

This work has been funded by the MICINN-TEC project TEC2011-28201-C02-01 and the CUR of the DIUE of the Autonomous Government of Catalonia and the European Social Fund. Data were provided by ESA in the frame of the AgriSAR 2009 campaign.

REFERENCES

[1] A. Alonso-Gonzalez, C. Lopez-Martinez, and P. Salembier. Filtering and segmentation of polarimetric sar images with binary partition trees. In *Proc. IEEE IGARSS*, pages 4043–4046, 2010.

[2] A. Alonso-Gonzalez, C. Lopez-Martinez, and P. Salembier. Binary Partition Tree as a polarimetric SAR data representation in the space-time domain. In *Proc. IEEE IGARSS*, pages 3819–3822, 2011.

[3] A. Alonso-Gonzalez, C. Lopez-Martinez, and P. Salembier. PolSAR speckle filtering and segmentation based on Binary Partition Tree representation. In *Proc. ESA PolInSAR*, 2011.

[4] A. Alonso-Gonzalez, C. Lopez-Martinez, and P. Salembier. Filtering and segmentation of polarimetric SAR data based on binary partition trees. *IEEE TGRS*, 50(2):593 –605, feb. 2012.

[5] A. Alonso-González, S. Valero, J. Chanussot, C. López-Martínez, and P. Salembier. Processing multidimensional SAR and hyperspectral images with binary partition tree. *Proceedings of the IEEE*, PP(99):1 –25, 2012.

[6] Frederic Barbaresco. Interactions between symmetric cone and information geometries: Bruhat-tits and siegel spaces models for high resolution autoregressive doppler imagery. In Frank Nielsen, editor, *Emerging Trends in Visual Computing*, volume 5416 of *Lecture Notes in Computer Science*, pages 124–163. Springer Berlin / Heidelberg, 2009.

[7] S. R. Cloude and E. Pottier. A review of target decomposition theorems in radar polarimetry. *IEEE Transactions on Geoscience and Remote Sensing*, 34(2):498–518, 1996.

[8] P. Salembier and L. Garrido. Binary partition tree as an efficient representation for image processing, segmentation, and information retrieval. *IEEE TIP*, 9(4):561–576, 2000.

[9] S. Valero, P. Salembier, J. Chanussot, et al. New hyperspectral data representation using binary partition tree. In *Proc. IEEE IGARSS*, 2010.